ACS OMEGA

Open Access

http://pubs.acs.org/journal/acsodf

Article

Assessing the Metabolic Variations of Invasive and Noninvasive Unilateral Retinoblastoma Patients

Khushboo Gulati, Krishna Mohan Poluri,* and Swathi Kaliki*

Cite This: *ACS Omega* 2024, 9, 40082−40094

Read Online

ACCESS | Metrics & More | Article Recommendations | Supporting Information

ABSTRACT: Retinoblastoma (Rb) is a pediatric eye cancer which if diagnosed at later stages can lead to Rb invasion into the choroid, optic nerve, sclera, or beyond, with the potential of undergoing metastasis. Cancer cells, including Rb cells, reprogram their metabolic circuits for their own survival and progression, which provides a great opportunity to monitor the extent of Rb progression based on metabolic differences. Henceforth, the present study aims to map the metabolic variations in patients with invasive (primarily enucleated eyes with high-risk histopathological features) and noninvasive (eyes salvaged with treatment) unilateral retinoblastoma (Rb) using nuclear magnetic resonance (NMR) based serum metabolomics. Quantification of differential metabolites in the serum obtained from 9 patients with invasive and 4 with noninvasive unilateral Rb along with 6 controls (no retinal pathology) was carried out using ^{1}H NMR spectroscopy. A total of 71 metabolites, such as organic acids, amino acids, carbohydrates, and others, were identified in the serum obtained from 9 patients with invasive and 4 with noninvasive unilateral Rb. Partial least-squares discriminant analysis (PLS-DA) models depicted distinct grouping of invasive and noninvasive Rb patients and controls. Differential metabolic fingerprints were observed for invasive and noninvasive Rb patients based on their biostatistical analyses with respect to controls. Remarkable perturbation was observed among various metabolites such as 4-aminobutyrate, 2-phosphoglycerate, *O*-phosphocholine, proline, Sn-glycero-3-phosphocholine (Sn-GPC), and *O*-phosphoethanolamine in noninvasive and invasive Rb patients with most of the effects being heightened in the latter group. Metabolic changes unique to invasive and noninvasive Rb patients were also observed. Multivariate receiver operating characteristics (ROC) analysis unveiled the highest accuracy and potency of ROC models 2 and 5 to distinguish the noninvasive and invasive Rb from controls, respectively. Metabolites identified in the serum of patients with invasive and noninvasive Rb may aid in advancing our knowledge about Rb tumor biology. Differential aberrant metabolic variations in patients with invasive Rb compared to those with noninvasive Rb may guide the decision of enucleation versus globe salvage.

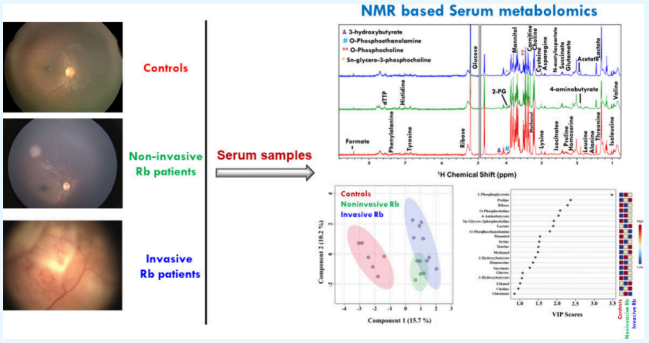

1. INTRODUCTION

Retinoblastoma (Rb) is an ocular malignancy which predominantly occurs in young children.[1] The occurrence rate of Rb is around 1 in every 16000−20000 live births worldwide.[2] Rb constitutes 3% of all the pediatric cancers and is mostly diagnosed below 5 years of age.[3] The root cause of Rb is hereditary/sporadic mutations in both alleles of the RB1 gene (first identified tumor suppressor gene) as explained by Knudson in the 1970s.[4] Hereditary Rb is an outcome of germline mutation in one allele followed by a sporadic mutation in another allele of the RB1 gene and is characterized by a multifocal-bilateral tumor. In contrast, sporadic Rb is a result of two separate somatic mutations in alleles of the Rb1 gene of developing retinal cells. Sporadic Rb patients mostly develop unifocal−unilateral tumors. It has been recognized that 60% of Rb cases are unilateral, and 15% of them are hereditary.[5] This indicates that all the nonhereditary cases are unilateral, although not all the unilateral cases are supposed to be nonhereditary.

Rb patients are also categorized into noninvasive and invasive Rb patients on the basis of their clinical behavior.[6] Noninvasive Rb patients exhibit tumors constricted within the retina and subretinal space, and vitreous and invasive Rb implies tumor invasion into the choroid, optic nerve, sclera, or beyond with the potential of undergoing metastasis.[7] Several prognostic and treatment modalities including enucleation, cryotherapy, chemotherapy, brachytherapy, intraarterial chemotherapy, intravitreal chemotherapy, and systemic chemotherapy have been developed for Rb over the past few decades.[8] Management of noninvasive Rb patients aims at

Received: June 28, 2024
Revised: August 8, 2024
Accepted: August 30, 2024
Published: September 12, 2024

vision/eye salvage. In contrast, the primary enucleation along with chemotherapy is carried out in invasive Rb patients owing to their high-risk histopathological features.[9] Invasive Rb patients are prone to metastasize tumors in distant organs and affect the survival rate.[10] Hence, there is a dire need for the early diagnosis of invasive Rb patients to facilitate their timely diagnosis and for optimal treatment decisions in order to save their vision/eye/life. On this note, it is imperative to assess the differential characteristic features of invasive Rb patients with respect to noninvasive Rb patients using a noninvasive screening strategy that will aid in the development of early diagnostic/prognostic markers for Rb invasion.

Serum based metabolomics is a noninvasive screening technique to scrutinize cancer patients on the basis of their distinct metabolic profiles.[11] It is based on the notion that cancer cells essentially reprogram their metabolic circuits for their survivability and progression.[12,13] Further, it has also been found that metabolic phenotypes evolve with tumor initiation and progression.[14] This has greatly attracted researchers across the globe to define degrees of cancer invasiveness by exploiting their distinct metabolic vulnerabilities. Numerous metabolic studies have indicated metabolite-specific aberrations among noninvasive and invasive versions of differential cancers including breast cancer, duct cancer, lung cancer, bladder cancer, etc.[15−17] Considering the importance of metabolites in tumor invasion and progression, it is imperative to perform systematic and thorough investigations of metabolic disparities among the Rb patients with varying degrees of tumor invasion.

Henceforth, the present study unraveled the metabolic differences among the noninvasive and invasive unilateral Rb patients using NMR based serum metabolomics with the aim to identify key metabolites involved in Rb invasion. The results depicted distinct metabolic profiles of noninvasive and invasive Rb patients with respect to controls. Interestingly, both invasive and noninvasive Rb patients showed synonymic patterns of expression of metabolites as compared to controls. However, the extent of metabolic perturbations was discrete among both Rb patients' subtypes. Further, univariate statistical analysis displayed metabolic aberrations that were unique for noninvasive and invasive Rb patients. Specific upregulation in the serum levels of ornithine, betaine, and glucose in noninvasive Rb patients and a unique upsurge of lactate, taurine, methanol, and pyruvate were observed in invasive Rb patients. Furthermore, biomarker investigations revealed a panel of metabolic features with high predictive diagnostic/prognostic value. Multivariate ROC analysis revealed the excellent power of ROC model 2 which combines the expression of 2-phosphoglycerate, 4-aminobutyrate, 2-hydroxybutyrate, ornithine, and *O*-phosphoethanolamine to distinguish noninvasive Rb patients from controls. Contrasting to this, ROC model 5 which combines the panel of 36 metabolic features displayed the highest predictive accuracy for distinguishing invasive Rb patients from controls.

Altogether, the snapshot of such metabolic differences among noninvasive and invasive Rb patients enhanced our understanding of the underlying mechanism of Rb invasion and laid the foundation for the development of future diagnostic/prognostic biomarkers for the timely and effective treatment of both noninvasive and invasive Rb patients.

2. RESULTS

2.1. Patient Demographical Features. The study included 13 unilateral Rb patients including 4 with noninvasive Rb and 9 with invasive Rb and 6 controls (NCs). The eyes with invasive Rb revealed high risk histological features including massive choroidal invasion (n = 3), postlaminar optic nerve invasion (n = 4), and extrascleral extension (n = 2) (Figure 1).

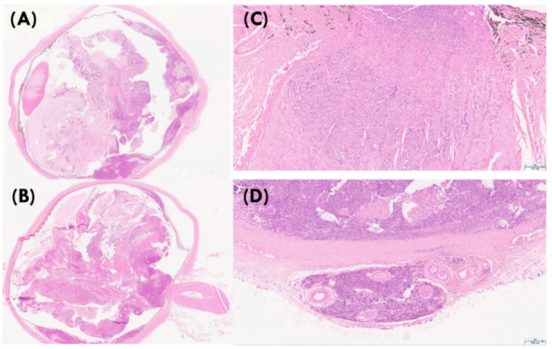

Figure 1. High-risk histopathological features in invasive retinoblastoma (Hematoxylin & Eosin stain). (A) Massive choroidal invasion, (B) massive multifocal choroidal invasion, (C) postlaminar optic nerve invasion, and (D) extra scleral tumor extension.

All of the invasive Rb patients had undergone primary enucleation for advanced Rb. Detailed demographic and clinical features of patients involved in the study are summarized in Table 1.

2.2. Exploring Metabolic Aberrations among Noninvasive and Invasive Rb Patients. NMR based serum metabolomics analysis was performed to assess the metabolic

Table 1. Demographic Details of All of the Rb Patients and Controls Involved in the Study along with Histopathological High-Risk Features in Those with Invasive Rb[a]

Sample	Sex (F/M)	Age (years)	Category (NRB/IRB)	Histopathology HRF (as indicated using HC)
Rb1	F	3	IRB	Extrascleral invasion
Rb2	M	3	IRB	Extrascleral invasion
Rb3	M	3	IRB	Massive choroidal invasion
Rb4	M	3	IRB	Massive choroidal invasion
Rb5	F	2	IRB	Post laminar optic nerve invasion
Rb6	F	2	IRB	Post laminar optic nerve invasion
Rb7	M	11 months	IRB	Post laminar optic nerve invasion
Rb8	F	6	IRB	Post laminar optic nerve invasion
Rb9	F	4	IRB	Massive choroidal invasion
Rb10	M	3 months	NRB	NA
Rb11	M	5	NRB	NA
Rb12	F	5 months	NRB	NA
Rb13	M	4	NRB	NA
C1	M	1	C	NA
C2	M	8	C	NA
C3	F	5	C	NA
C4	M	6 months	C	NA
C5	F	5	C	NA
C6	F	9	C	NA

[a]Abbreviations used are as follows. NRB: noninvasive Rb and IRB: invasive Rb patients, C-controls, HRF: High Risk features, HC: histochemistry, NA: not applicable.

https://doi.org/10.1021/acsomega.4c06014
ACS Omega 2024, 9, 40082−40094

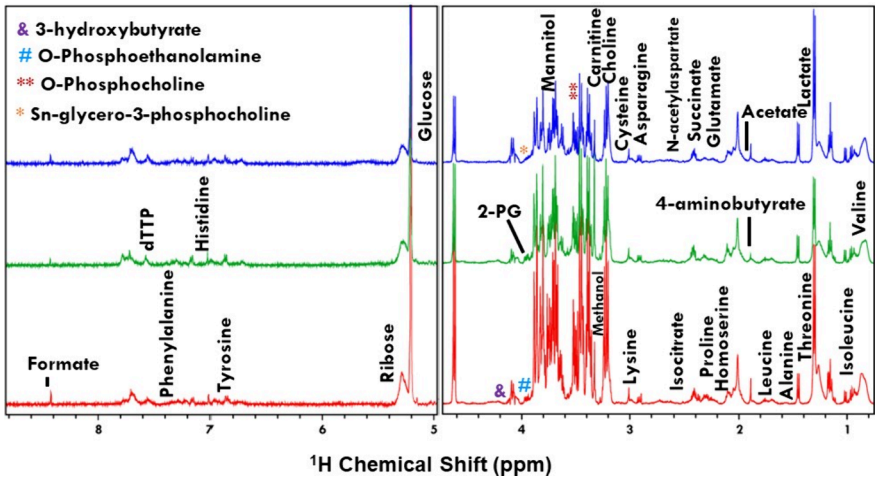

Figure 2. Schematic representing the stack of ^{1}H NMR spectra obtained for serum samples from (A) noninvasive (blue), (B) invasive (green) Rb patients, and (C) controls (red). Assigned metabolites are highlighted. Water region from δ 4.6 to 4.9 ppm is omitted from each spectrum to increase the spectral resolution. The following abbreviations used are as follows: 2-PG, 2-phosphoglycerate.

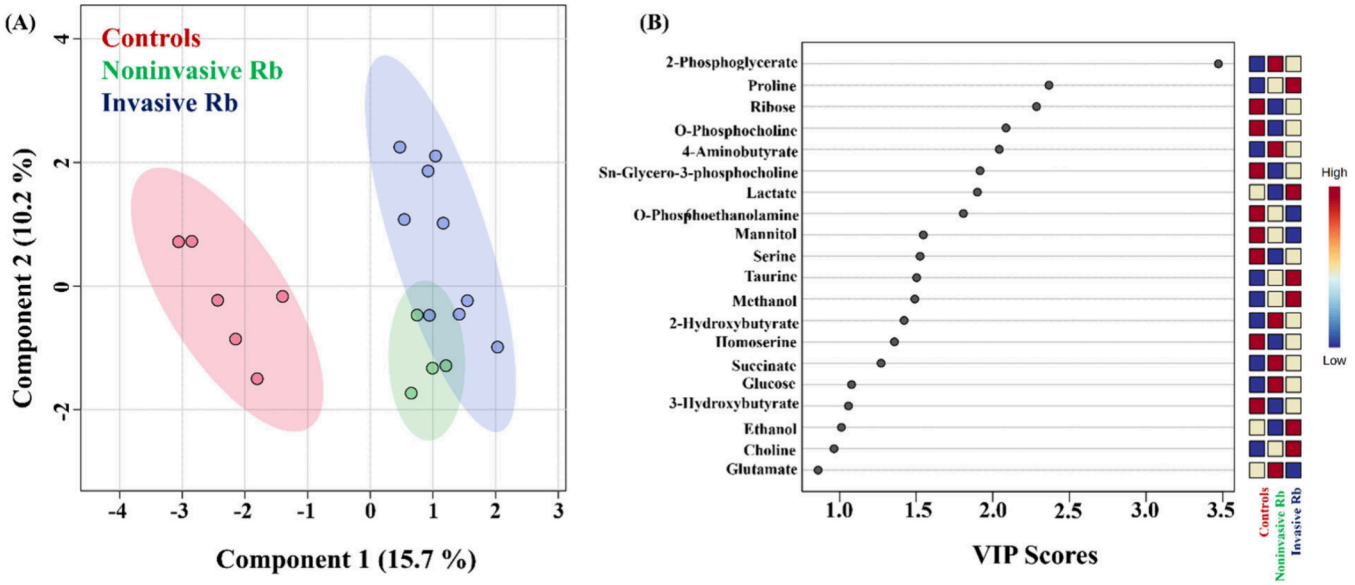

Figure 3. Multivariate statistical analysis of controls, noninvasive, and invasive Rb patients. (A) Representative partial least-squares discriminant (PLS-DA) score plot generated on the basis of a concentration data set of 71 metabolites assigned in the ^{1}HNMR spectra of serum from controls, noninvasive, and invasive Rb patients. Semitransparent ovals red (controls), green (noninvasive), and blue (invasive) represent a 95% confidence interval. (B) VIP score plot depicting the significantly discriminatory metabolites among noninvasive and invasive Rb patients with respect to controls. Three lines of vertical boxes on the right display metabolic variations in controls and noninvasive and invasive Rb patients.

variations among noninvasive and invasive unilateral Rb patients with respect to controls (NC). Further, perturbations in metabolic pathways associated with both noninvasive and invasive Rb patients were unraveled. Additionally, attempts were also made to identify diagnostic markers for both noninvasive and invasive Rb patients.

2.2.1. Analyzing the Circulatory Metabolites in Sera of Noninvasive and Invasive Rb Patients. CPMG NMR spectra for each serum sample were annotated with a metabolite as per their chemical shift assignment. 71 distinct metabolites belonging to different categories including carbohydrates, organic acids, amino acids, and their derivatives, nucleic acids, and others were assigned based on chemical shift data of differential metabolites available in the human metabolome database and 500 MHz metabolite spectral library present in Chenomx. A stack of CPMG spectra for invasive Rb, noninvasive Rb, and control with a few metabolite annotations is shown in Figure 2.

Unsupervised statistical analysis (PCA analysis) was performed using a normalized metabolite concentration data set to obtain an initial trend of different groups. Both 2D and 3D PCA score plots depict distinct groups of controls and Rb patients. Under chosen conditions, an optimal separation between noninvasive and invasive Rb patients was not observed. Hence, supervised statistical analysis (PLSDA) was carried out. The PLSDA score plot displayed distinct clusters of both invasive and noninvasive Rb patients and controls, which clearly implies the metabolic differences among different study groups (Figure 3A). This was further confirmed by the statistical significance measures (R^2 = 0.96, Q^2 = 0.52) obtained as a result of 5-fold cross validation of the attained PLSDA model (Figure S1). Based on the PLSDA model,

https://doi.org/10.1021/acsomega.4c06014
ACS Omega 2024, 9, 40082−40094

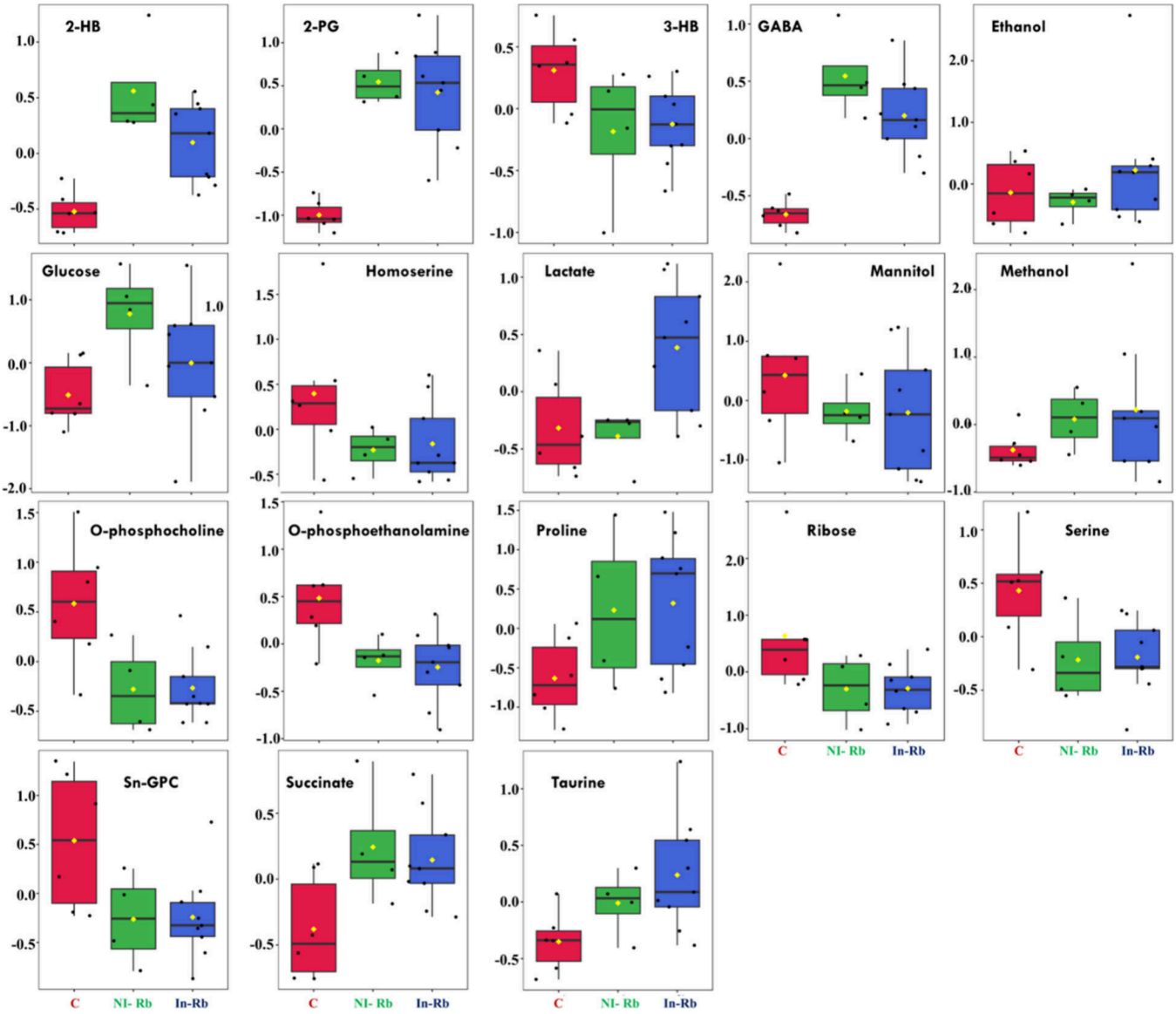

Figure 4. Box cum whisker plots of the most compelling serum metabolites differentiating noninvasive and invasive Rb patients from controls. Each box represents a significantly distinct metabolite obtained using VIP score plot analysis performed on the basis of the PLSDA model generated for controls versus noninvasive and invasive Rb patients. In a given box plot, the horizontal line within the box, top, and bottom borders represents the median, 75th, and 25th percentiles, respectively, while upper and lower whiskers display the 95th and 5th percentiles, respectively. The following abbreviations were used: 2-HB: 2-hydroxybutyrate, 2-PG: 2-phosphoglycerate, 3-HB: 3-hydroxybutyrate, GABA: 4-aminobutyrate, Sn-GPC: Sn-glycero-3-phosphocholine.

circulatory metabolites with high potency of discrimination between noninvasive and invasive Rb patients from controls were identified using a variable of importance (VIP) score plot analysis (Figure 3B). Metabolites possessing VIP scores more than 1.0 are contemplated as discriminatory features significantly contributing toward the obtained discriminatory model. In contrast to NCs, sera of noninvasive and invasive Rb patients showed irregularities in the level of 18 metabolites including 2-phosphoglycerate, proline, ribose, *o*-phosphocholine, 4-aminobutyrate, *sn*-glycero-3phosphocholine, lactate, *o*-phosphocholine, mannitol, serine, taurine, methanol, 2-hydroxybutyrate, homoserine, succinate, glucose, ethanol, and 3-hydroxybutyrate (Figure 3B).

Further, quantitative variations of metabolites among noninvasive and invasive Rb patients with respect to controls were assessed using the Box cum Whisker plots as shown in Figure 4. These box plots provided a clear view of up or down regulation patterns of specific metabolites in noninvasive/invasive Rb patients. Metabolites including 2-phosphoglycerate, glucose, lactate, succinate, taurine, 2-hydroxybutyrate, GABA, proline, and methanol showed an upregulation in the sera of Rb patients, while mannitol, ribose, *o*-phosphocholine, *o*-phosphoethanolamine, *sn*-glycerophosphocholine (Sn-GPC), serine, 3-hydroxy butyrate, homoserine, and serine displayed lower expression in Rb patients. Interestingly, a similar pattern of up-/downregulation of metabolites has been exhibited by noninvasive and invasive Rb subgroups. However, the extent of such metabolic variations among noninvasive and invasive Rb patients is quite distinct, indicating unequivocal metabolic disturbances associated with invasiveness of the disease. Heat maps were generated for the 25 topmost significantly discriminatory features providing an overall snapshot of

https://doi.org/10.1021/acsomega.4c06014
ACS Omega 2024, 9, 40082−40094

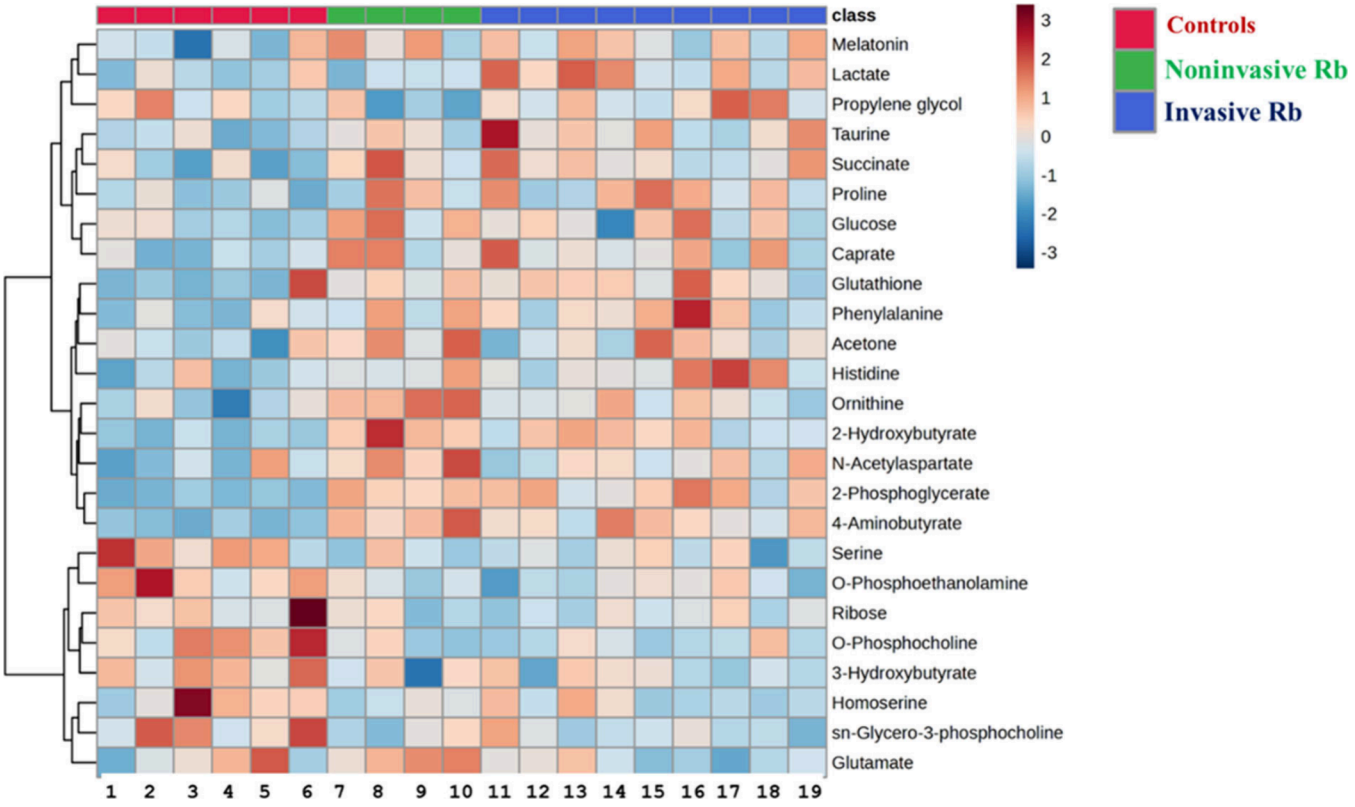

Figure 5. Heat map displaying an overview of metabolic variations of the top 25 distinct metabolites in serum from controls, noninvasive, and invasive Rb patients. The *X* axis displays serum samples from controls (Lanes 1−6), noninvasive (Lanes 7−11), and invasive (Lanes 12−19) Rb patients. Color variation displays the variation in metabolite concentration, with dark blue and dark red colors specifying the most elevated and the most reduced metabolic concentrations. Level of significance (p-value) for the metabolite was set to ≤0.05.

metabolic aberrations associated with Rb patients' subgroups (Figure 5). Heat maps clearly revealed distinct metabolic expression profiles among sera from noninvasive and invasive Rb subgroups in contrast to controls. Overall, 8 metabolites showed low expression in Rb patients, while higher expression was marked among the remaining 17 metabolites in sera from Rb subgroups as compared to NCs (Figure 5). These metabolic variations are consistent with those obtained using PLS-DA analysis.

Additionally, fold change analysis was also carried out for distinct subgroups including noninvasive Rb versus controls and invasive Rb versus controls with an aim to identify the significant metabolic alterations with fold change threshold value ≥1.4 and level of significance, p-value, <0.05. Sixteen metabolites with FC value ≥1.4 were observed that were common among both Rb patient subgroups. Metabolites including 2-phosphoglycerate, GABA, 2-hydroxybutyrate, proline, caprate, asparagine, and succinate were found to be elevated in both noninvasive and invasive Rb patients. Contrastingly, *o*-phosphocholine, *o*-phosphoethanolamine, *sn*-glycerophosphocholine, homoserine, ribose, mannitol, and serine showed significant depletion in sera of both Rb subgroups (Table 2). Noninvasive Rb patients displayed specific upregulation in the levels of ornithine, betaine, and glucose with fold change values of 2.23, 1.52, and 2.07, respectively. In sharp contrast, a unique upsurge in the serum levels of lactate, taurine, methanol, and pyruvate was markedly prominent in invasive Rb patients (Table 2). Altogether, this implies that both noninvasive and invasive Rb patients share the pattern of metabolic distortions discriminating Rb patients from NCs. However, there are some metabolic specificities associated with degrees of severity of the disease as dictated by the metabolic modulations that solely belong to the noninvasive/invasive Rb patients.

2.2.2. Decoding the Metabolic Pathways Disturbed in Noninvasive and Invasive Rb Patients. We sought to determine the metabolic pathways specifically disturbed in noninvasive and invasive Rb patients. Hence, pairwise pathway impact analysis has been performed for noninvasive Rb patients and invasive Rb patients with respect to controls (Figure 6). Both noninvasive and invasive Rb patients showed perturbation in 48 metabolic pathways (Tables S1 and S2); the most significantly disturbed metabolic pathways with −log 10(p) value >0.5 and pathway impact value >0.1 were quite different among both Rb subgroups. Both noninvasive and invasive Rb patients shared significant disturbance among 7 metabolic pathways including (1) butanoate metabolism, (2) arginine and proline metabolism, (3) alanine, aspartate, and glutamate metabolism, (4) glutathione metabolism, (5) glycerophospholipid metabolism, (6) cysteine and methionine metabolism, and (7) taurine and hypotaurine metabolism. Although both noninvasive and invasive Rb patients displayed similar pathway impact values (corresponding to pathway topology), −log 10(p) values, which directly correlate with pathway enrichment, were quite distinct for commonly perturbed metabolic pathways (Table 3). These changes imply the signatory metabolic perturbations pertaining to unilateral Rb patients regardless of their Rb invasion status.

Apart from these common pathways, both Rb subgroup patients displayed distortions in specific metabolic pathways.

https://doi.org/10.1021/acsomega.4c06014
ACS Omega 2024, 9, 40082−40094

Table 2. Summary of Discriminatory Metabolites among Noninvasive (NI) and Invasive (IN) Rb Patients with Respect to Controls (Ctrls) as Assessed Using a Univariate Fold Change Analysis[A]

S. No.	Metabolites	Relative Fold Change	
		Ctrls vs NI_Rb	Ctrls vs IN_Rb
1	2-Phosphoglycerate	3.31	3.16
2	*o*-Phosphocholine	0.32	0.32
3	4-Aminobutyrate	2.89	2.26
4	2-Hydroxybutyrate	2.49	1.78
5	Ornithine	2.23	-
6	Proline	2.15	2.25
7	*o*-Phosphoethanolamine	0.48	0.45
8	Glucose	2.07	-
9	*sn*-GPC	0.49	0.50
10	Homoserine	0.55	0.60
11	Ribose	0.55	0.55
12	Caprate	1.77	1.54
13	Mannitol	0.58	0.65
14	Succinate	1.71	1.58
15	Asparagine	1.71	1.23
16	Serine	0.59	0.60
17	Betaine	1.52	-
18	Lactate	-	1.95
19	Taurine	-	1.64
20	Methanol	-	1.57
21	Pyruvate	-	1.54

[A]The threshold fold change value was set to 1.5, and log 2(FC) values with p-value ≤ 0.05 were taken into consideration. Fold change values greater than 1 and less than 1 of the metabolites implies their elevation and depreciation, respectively, in the serum of Rb patients' subtypes.

Noninvasive Rb patients reflected prominent disturbance in pathways related to starch and sucrose metabolism, galactose metabolism, tryptophan metabolism, and arginine biosynthesis. Interestingly, six additional metabolic pathways including (1) glycine, serine, and threonine metabolism, (2) phenylalanine, tyrosine, and tryptophan biosynthesis, (3) phenylalanine metabolism, (4) histidine metabolism, (5) glycolysis/gluconeogenesis, and (6) pyruvate metabolism marked specific dysregulation among invasive Rb patients (Table 3). Such a distinct observation evidently points toward the association of severe metabolic disturbances associated with the advancement of disease in invasive Rb patients. Altogether, both multivariate/univariate analysis and pathway impact analysis revealed the pattern of both shared and specific metabolic distortions associated with noninvasive and invasive Rb patient subgroups. This exquisitely confirms that the degrees of metabolic aberrations are highly specific to the underlying pathophysiological conditions of the Rb patients' subgroups.

2.2.3. Evaluating Serum Metabolic Profiles as a Diagnostic Tool for Noninvasive and Invasive Rb Patients. The potential of serum metabolic profiles as diagnostic biomarkers to distinguish noninvasive and invasive Rb patients from controls was assessed by using both multivariate and classical univariate receiver operating characteristic (ROC) analysis.

Multivariate ROC analyses demonstrate the potential of the combination of metabolic features as diagnostic biomarkers. For noninvasive Rb patients versus controls, multivariate ROC analysis displayed 5 models while taking into consideration the combination of 3, 5, 10, 20, 36, and 71 metabolic features, respectively. The second ROC model that was generated using a combination of 5 metabolic features displayed the highest AUC value (0.97) with a confidence interval (CI) of (0.66−1) (Figure 7A) along with the highest predictive accuracy (92.5%) (Figure 7B). The top 15 metabolic features along with their frequency generated on the basis of the ROC model are shown in Figure 7C. ROC model 2 implies the excellent ability of the combination of 2-phosphoglycerate, 4-aminobutyrate, 2-hydroxybutyrate, ornithine, and *o*-phosphoethanolamine to distinguish noninvasive Rb patients from controls. Additionally, multivariate analysis for invasive Rb patients with respect to controls revealed the fifth model which considers the panel of 36 metabolic features possessing the highest AUC value (0.97), confidence interval of 0.9 to 1.0, and predictive accuracy of 92%, making this the best ROC model (Figure 8A−C). The top 36 metabolic features, a combination of which has high discriminating potency among invasive Rb patients and controls, are displayed in Figure 8C. Multivariate ROC analysis for noninvasive Rb versus invasive Rb patients revealed the third ROC model (AUC: 0.68, CI: 0.03−1) as the best model, which combines 10 metabolic features for differentiating the Rb subgroups (Figure S2A−C). This model with predictive accuracy of 57.1% is modest to distinguish Rb subgroup patients.

Further, classical univariate ROC analysis was also carried out to determine the potency of individual circulatory metabolites in serum to serve as diagnostic biomarkers for Rb patient subgroups. ROC curves of metabolites including 2-phosphoglycerate, 2-hydroxybutrate, GABA, ornithine, glucose, ascorbate, tryptophan, and *N*-acetyl aspartate with AUC values >0.9 displayed high power to discriminate noninvasive Rb patients from controls (Figure S3). In contrast, metabolic features including 2-phosphoglycerate (AUC: 1, 95% CI: 1−1), GABA (AUC: 1, CI: 1−1), 2-HB (AUC: 0.98, 95% CI: 0.8−1), tryptophan (AUC: 0.94, 95% CI: 0.73−1), and *o*-phosphocholine (AUC: 0.92, 95% CI: 0.74−1) reflected their potential to differentiate invasive Rb patients (Figure S4). The discriminatory metabolic features (2-phosphoglycerate, GABA, 2-HB, and tryptophan) are common among both noninvasive and invasive Rb patients; hence, speculating these individual metabolic variations is an unreliable means for diagnosing invasive Rb patients. This clearly suggests that it is essential to consider the panel of metabolic features for monitoring the invasiveness of a tumor in Rb patients. Additionally, univariate ROC analysis to distinguish noninvasive and invasive Rb patients was also performed. Metabolites including glutamate (AUC: 1, 95% CI: 0.88−1), ornithine (AUC: 1, 95% CI: 0.88−1), *N*-acetylaspartate (AUC: 0.88, 95% CI: 0.59−1), lactate (AUC: 0.83, 95% CI: 0.55−1), propylene glycol (AUC: 0.83, 95% CI: 0.41−1), alanine (AUC: 0.80, 95% CI: 0.41−1), and GABA (AUC: 0.80, 95% CI: 0.44−1) were found to possess distinctive potency for Rb patient subgroups (Figure S5). Among these metabolites, the elevated levels of lactate, propylene glycol, and alanine and decreased levels of glutamate, ornithine, *N*-acetyl aspartate, and GABA were observed in sera from invasive Rb patients in contrast to that from noninvasive Rb patients, which is in line with previously defined univariate (fold change) and multivariate (PLSDA) analysis. Altogether, these results suggest that these metabolic features may serve as valuable diagnostic/prognostic tools for screening Rb patients' subgroups.

https://doi.org/10.1021/acsomega.4c06014
ACS Omega 2024, 9, 40082−40094

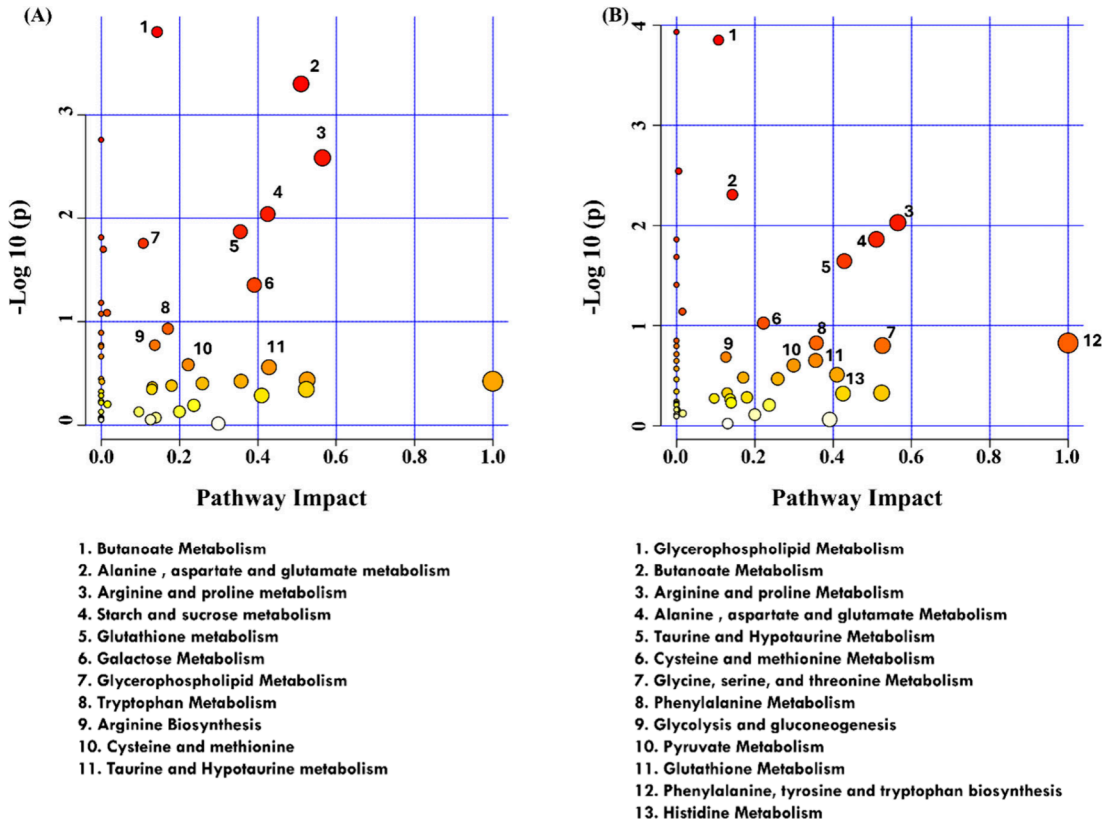

Figure 6. Pathway impact analysis of (A) noninvasive and (B) invasive Rb patients with respect to controls. Each circle represents the metabolic pathway perturbed as a result of metabolic aberration associated with Rb patient subtypes. The vertical and horizontal axis represents −log 10(p) and pathway impact values, respectively. −Log 10(p) corresponds to pathway enrichment, variation of which is indicated by the gradient of node colors ranging from red to yellow. Pathway impact value is related to topological features of the metabolic pathway and is directly proportional to the diameter of circular nodes.

3. DISCUSSION

Metabolic heterogeneity is a hallmark for all cancer types, including Rb. Rb cells, like other cancer cells, rewire their metabolic circuit to meet the increasing bioenergetic demands to support their cellular growth and progression.[13,18] It is well established that metabolic vulnerabilities evolve along the axis of tumor progression.[18,19] Hence, it is speculated that metabolic fuel requirements are quite distinct among the noninvasive and invasive versions of Rb. Exploring the metabolic evolutionary trajectory across distinct Rb patients' subgroups provides new avenues for the early diagnostic and prognostic markers associated with Rb invasion. Recent work on serum based metabolic profiling of Rb patients provided a snapshot of metabolic differences among unilateral and bilateral Rb patients.[20] To the best of our knowledge, none of the studies have focused on studying the metabolic disturbances associated with Rb invasion using serum samples. Hence, elucidation of the metabolic evolution from noninvasive to invasive Rb with the aim to identify noninvasive diagnostic and prognostic markers for distinct Rb patients is an aspect of clinical significance.

In the current study, attempts were made to get insights into the metabolic fingerprints specific to noninvasive and invasive Rb while providing a glimpse of the metabolic evolutionary mechanism underlying the invasion of Rb. Detailed analysis revealed distinct levels of aberration in circulating metabolites in serum from noninvasive and invasive Rb patients (Figure 9). Major metabolites commonly perturbed among both subgroups include 2-phosphoglycerate, lactate, 4-aminobutyrate, *o*-phosphoethanolamine, *o*-phosphocholine, *sn*-glycerophosphocholine, and proline. Disturbed levels of ornithine and betaine were marked in noninvasive Rb patients, while pyruvate, lactate, and taurine showed unique alterations in invasive Rb patients. Additionally, the perturbation in metabolic pathways specific to both Rb subgroups along with 9 commonly altered pathways related to amino acids and membrane metabolites were also identified. Around 7 metabolic pathways specifically in invasive and 2 in noninvasive Rb patients were found to be disturbed with respect to controls. Interestingly, higher metabolic abnormalities were observed among invasive Rb patients, thus highlighting the severity of disease in invasive Rb patients with a high propensity to undergo metastasis. The implications of such metabolic differences reflected in noninvasive and invasive Rb phenotypes are discussed in detail.

Alterations in the circulating metabolites related to energy metabolic pathways, including glucose, mannitol, ribose, lactate, and succinate, were observed in both invasive and noninvasive Rb patients. Lower levels of mannitol and ribose imply their utilization to meet energy requirements. Increased 2-phosphoglycerate, a glycolytic pathway intermediate, implies that sugars are undergoing glycolysis. However, due to the dampened glycolytic pathway in Rb patients as mentioned by previous reports,[21] sugars are not completely metabolizing which supports the observation of increased 2-phosphoglycerate levels in the serum of both noninvasive and invasive Rb patients. Contrary to this, particularly invasive Rb patients

https://doi.org/10.1021/acsomega.4c06014
ACS Omega 2024, 9, 40082−40094

Table 3. Comparative Analysis of Significantly Perturbed Metabolic Pathways (−log 10(p) Values ≥0.5 and Pathway Impact Value >0.1) among Noninvasive and Invasive Rb Patients with Respect to Controls

		Noninvasive Rb patients vs controls		Invasive Rb patients vs controls	
S. No.	Metabolic pathways perturbed	−log 10(p)	Impact	−log 10(p)	Impact
1	Glycerophospholipid metabolism	1.76	0.11	3.85	0.11
2	Butanoate metabolism	3.80	0.14	2.31	0.14
3	Arginine and proline metabolism	2.58	0.57	2.03	0.57
4	Alanine, aspartate, and glutamate metabolism	3.30	0.51	1.86	0.51
5	Taurine and hypotaurine metabolism	0.56	0.43	1.64	0.43
6	Cysteine and methionine metabolism	0.58	0.22	1.03	0.22
7	Phenylalanine, tyrosine, and tryptophan biosynthesis	-	-	0.83	1.00
8	Phenylalanine metabolism	-	-	0.83	0.36
9	Glycine, serine, and threonine metabolism	-	-	0.80	0.53
10	Glycolysis/gluconeogenesis	-	-	0.69	0.13
11	Glutathione metabolism	1.87	0.36	0.65	0.36
12	Pyruvate metabolism	-	-	0.60	0.30
13	Histidine metabolism	-	-	0.51	0.41
13	Starch and sucrose metabolism	2.04	0.43	-	-
14	Galactose metabolism	1.35	0.39	-	-
15	Tryptophan metabolism	0.93	0.17	-	-
16	Arginine biosynthesis	0.77	0.14	-	-

showed lower glucose and higher lactate levels. This implies that in the case of invasive Rb glucose undergoes complete glycolysis, and pyruvate is converted into lactate, even in aerobic conditions, which is consistent with previous reports on other solid tumors.[22−24] In general, normal body cells convert glucose into lactate, especially under anaerobic conditions. In contrast, cancer cells preferentially metabolize glucose to lactate even under aerobic conditions, which is known as Warburg's effect/aerobic glycolysis.[25,26] This is the characteristic feature of many solid tumors including glioma, breast, head, and neck cancer.[22−24] Elevated lactate levels initiate acidosis in the tumor microenvironment, thereby promoting tumor invasion and metastasis of solid tumors.[27] A lower level of rise in 2-phosphoglycerate is marked in invasive Rb patients as compared to noninvasive Rb patients. This indicates that the glycolytic pathway may not be completely attenuated in the case of invasive Rb patients so as to fulfill their requirements of lactate to promote tumor invasion and immunosuppression. Elevated succinate, a TCA cycle intermediate, has been marked in both noninvasive and invasive Rb patients. Extracellular succinate is known to augment cancer growth, angiogenesis, metastasis, and immune evasion using SUCNR-1 mediated signaling pathways.[28] Serum succinate has been suggested as an important biomarker for lung cancer.[29] Elevated pyruvate levels were specifically observed in invasive Rb patients, indicating significant mitochondrial metabolic perturbations linked with invasion of Rb. Pyruvate, a master fuel for the TCA cycle, is obtained as an end product of glycolysis and additionally via multiple resources in cells.[30] Thus, perturbations in pyruvate levels in serum can be correlated to invasive Rb patients with an increased energy burden.

Decreased levels of *o*-phosphoethanolamine, *o*-phosphocholine, and *sn*-glycerophosphocholine were observed in sera from noninvasive and invasive Rb patients. This implies the disturbance of the glycerophospholipid pathway, perturbation of which has been marked in many cancer types.[31,32] Both *o*-phosphoethanolamine and *o*-phosphocholine, being the precursors of phosphatidylethanolamine and phosphatidylcholine, participate in the synthesis of membranes required for cancer cell proliferation. *sn*-Glycerophosphocholine, which is known to makeover the declined levels of choline, was found to be downregulated. This depicts its conversion into choline, a precursor of glycerophospholipids, imperative constituents in biological membranes.[33]

Serum levels of amino acids and their derivatives including proline, serine, homoserine, taurine, and GABA were found to be disturbed in both noninvasive and invasive Rb patients. Amino acids are key players in cell signaling events, protein synthesis, and nucleotide biosynthesis and also act as energy sources. Dysregulation of circulatory levels of amino acids supports cancer growth and metastasis. Proline is known to regulate the crosstalk between cancer cells and the tumor microenvironment (TME). Secreted proline is correlated to tumor progression owing to its involvement in collagen synthesis, a major component of the extracellular matrix (ECM) in the tumor microenvironment.[34] Higher fold change of proline in invasive than in noninvasive Rb patients implies the distinguished role of proline in tumor invasion/metastasis in an invasive Rb phenotype. Meanwhile, decreased levels of serine and homoserine were observed in both of the Rb subgroups. Serine serves as a source of carbon in one-carbon metabolism, which results in biosynthesis of lipids, proteins, and nucleic acids via a series of complex chemical reactions.[35,36] Indeed, homoserine is an intermediate in the biosynthesis of threonine, methionine, and isoleucine. Further, perturbed glutamate levels were observed in invasive Rb patients which might be pointing toward its utilization in the synthesis of other biomolecules required for cancer growth and progression. Glutamate is an important amino acid that is involved in the synthesis of α-keto acids through its carbon skeleton to meet ATP and fatty acid requirements, and its nitrogen is used for purine and pyrimidine synthesis. Additionally, glutamate acts as a precursor of proline, ornithine, and arginine and aids in the synthesis of other nonessential amino acids via Kerb's cycle. Importantly, glutamate is also a precursor of glutathione which is an imperative antioxidant that is used by the cancer cells to scavenge the highly elevated free radical species to further promote cancer cell growth and progression.[37]

An increased amount of taurine in invasive Rb patients is in accordance with a previous study by Kohe et al., who correlated the high taurine levels with highly differentiated invasive Rb phenotype.[38] It is interesting to note the increased secreted forms of GABA in both Rb patient subtypes, in contrast to controls. Elevated GABA levels correlate with the prevalence of immune-suppressive activities, halting the CD8+ T cell penetration in the tumor microenvironment. Moreover, GABA is also known to activate GABA receptors present on tumor cells, which triggers β-catenin signaling and promotes tumor growth.[39−44] Intriguingly, invasive Rb patients displayed lower levels of GABA than noninvasive Rb, implying the utilization of GABA in metastasizing the tumor cells to other

https://doi.org/10.1021/acsomega.4c06014
ACS Omega 2024, 9, 40082−40094

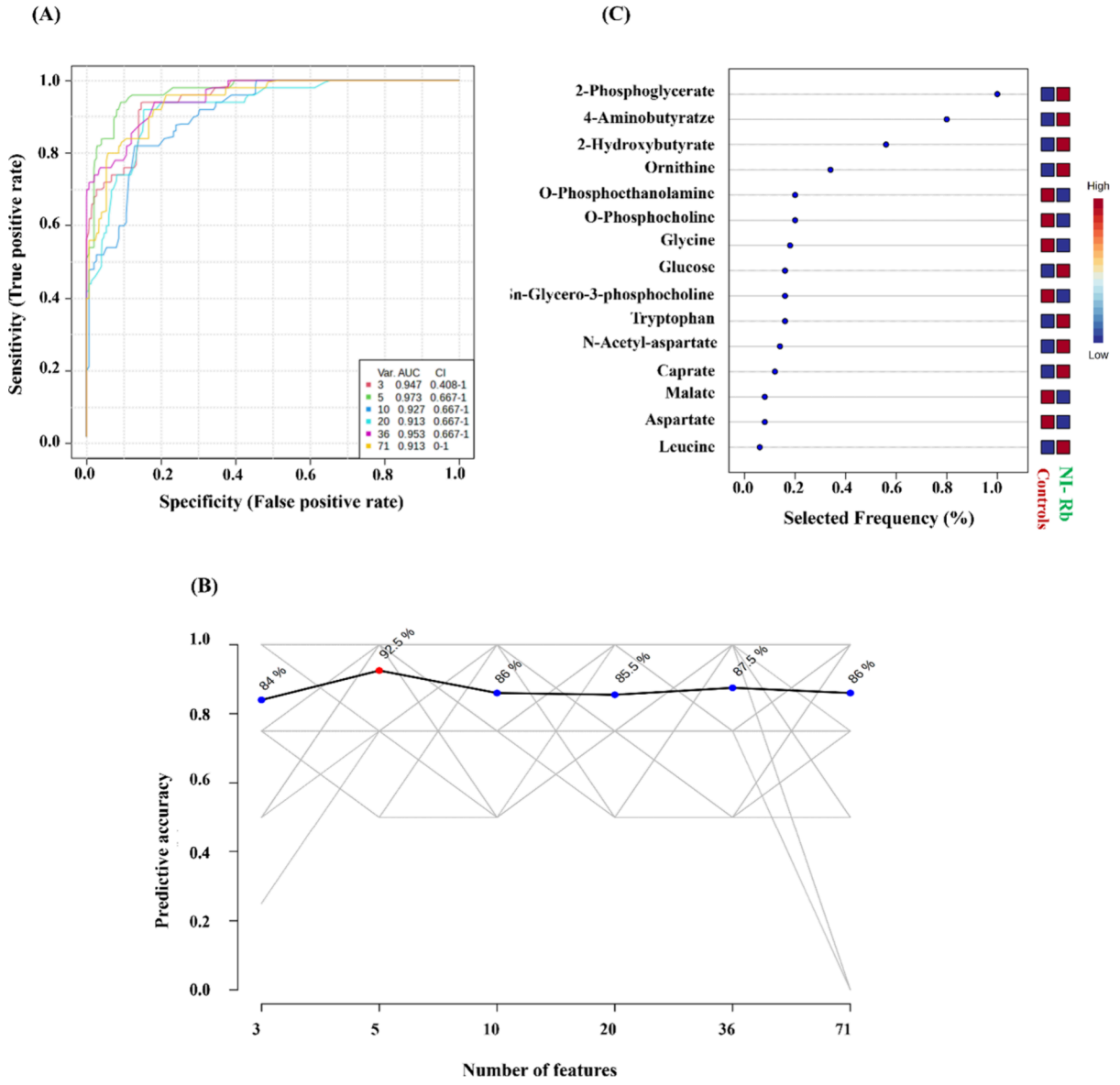

Figure 7. Multivariate ROC analysis to assess the diagnostic potency of automated selected metabolic features for differentiating noninvasive Rb patients from controls. (A) ROC curves were averaged from all cross validation (CV) runs. AUC (area under ROC curves) and CI (confidence interval) values for each ROC model are mentioned in inset (B) predictive accuracy for each ROC model based on the combination of distinct metabolic features. The highest predictive accuracy is highlighted with a red node. Top 5 metabolic features (along with frequency) used for the predictive model 2 (best model) are shown (C).

parts of the eye, which is consistent with the reports marking the importance of GABA in metastasis of cancerous cells.[45]

Elevated levels of ornithine have been observed specifically among noninvasive Rb patients. Ornithine is obtained as a byproduct of enzymatic conversion of arginine into urea and ornithine. Ornithine is metabolized by ornithine decarboxylase (ODC) to synthesize polyamines including spermidine, putrescine, or spermine, which in turn facilitates tumor growth and progression.[46] A growing body of evidence demonstrates the close association of elevated arginase levels and their downstream metabolites with the tumor progression.[47] ODC silencing using siRNA in human Y79 retinoblastoma cells showed significant reduction in polyamine synthesis and was suggested as a therapeutic target for Rb.[48]

Increased serum betaine observed in noninvasive Rb patients agrees with the study that showed the patients with elevated betaine levels are at high risk of cancer development.[49] The major sources of betaine in the body are diet as well as endogenous synthesis via oxidative conversion of choline into betaine aldehyde via mitochondrial choline dehydrogenase followed by the oxidation of betaine aldehyde to betaine through betaine aldehyde dehydrogenase.[50] Accumulation of betaine in serum due to excess endogenous synthesis/dietary intake has been associated with increased incidence of cancer by Xie et al.[49] However, heterogeneous serum betaine levels have been observed among distinct cancer types.[51−54] Further, ROC analysis confirmed that the panel of metabolites serves as a better diagnostic marker for the detection of invasive Rb patients as compared to individual metabolites for diagnosing noninvasive Rb patients. Collectively, our study provides a metabolic landscape pertaining to noninvasive and invasive Rb patients and thereby enhances our understanding of metabolic

https://doi.org/10.1021/acsomega.4c06014
ACS Omega 2024, 9, 40082−40094

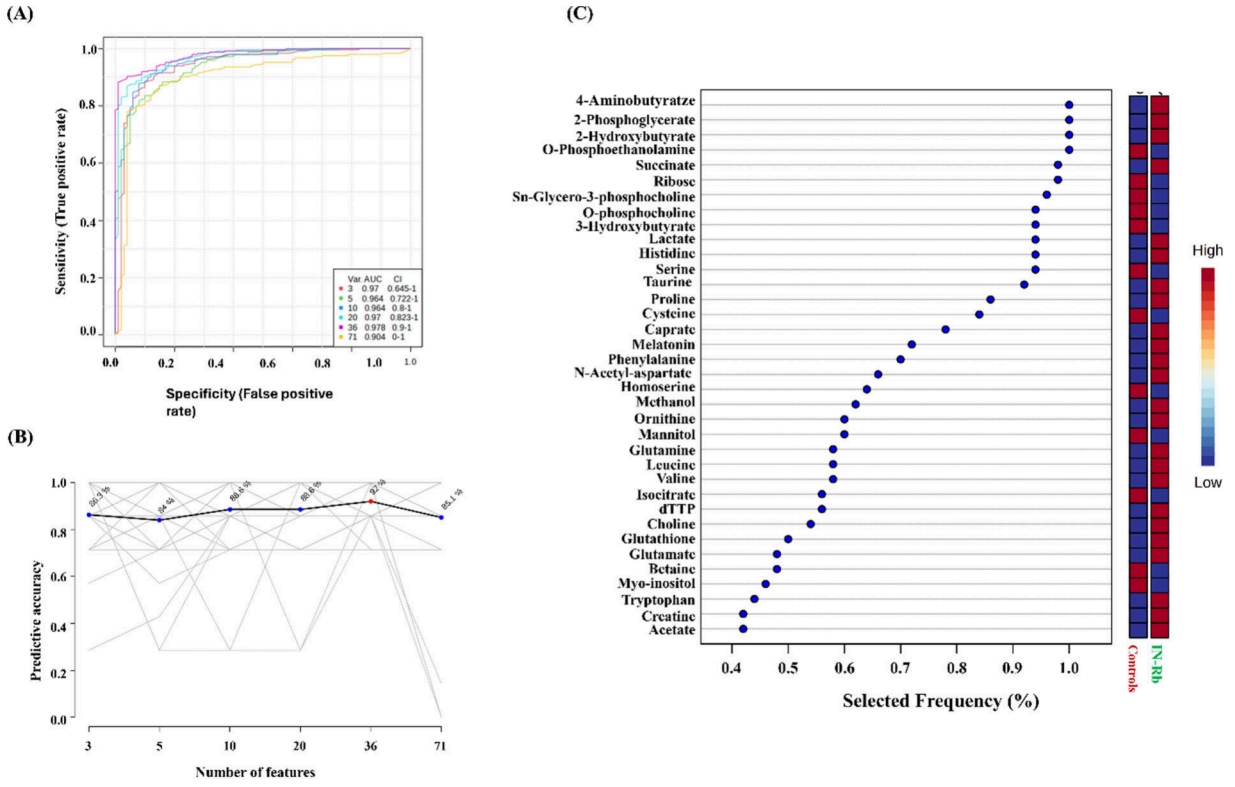

Figure 8. Multivariate ROC analysis to assess the diagnostic potency of automated selected metabolic features for differentiating invasive Rb patients from controls. (A) ROC curves averaged from all cross validation (CV) runs. AUC (area under ROC curves) and CI (confidence interval) values for each ROC model are mentioned in (B) predictive accuracy for each ROC model based on the combination of distinct metabolic features, and the highest predictive accuracy is highlighted with a red node. The top 36 metabolic features (along with frequency) used for the predictive model 5 (best model) are shown in (C).

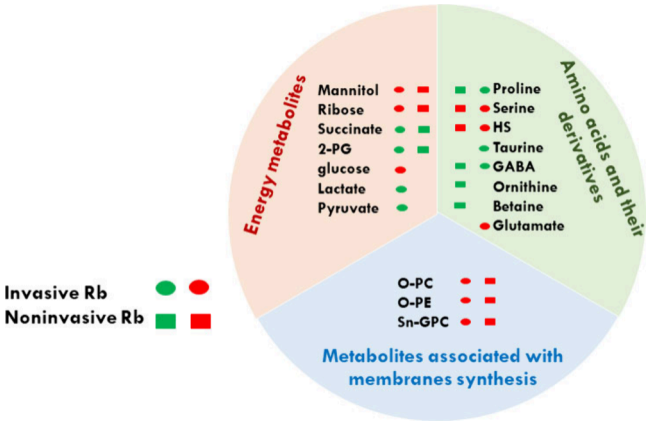

Figure 9. Schematic illustration of the metabolites perturbed in invasive and noninvasive Rb patients with respect to controls. Green and red colors indicate upregulation and downregulation of metabolites, respectively. Abbreviations used are as follows: HS: Homoserine, GABA: γ-aminobutyrate, O-PC: *o*-phosphocholine, O-PE: *o*-phosphoethanolamine, Sn-GPC: *sn*-glycerophosphocholine.

disturbances associated with invasive progression of Rb and provides opportunities to translate basic research to precisely design diagnostics, prognostics, and therapeutic measures for the disease.

4. CONCLUSIONS

This study aided in gaining insights into the potent metabolites and their associated metabolic pathways that play key roles in Rb tumor invasion and progression. Metabolic assessment across noninvasive and invasive Rb patients is essential to provide novel therapeutic targets to block Rb progression and invasion to the central nervous system and metastasis to the distant organs. Differential metabolic profiles of noninvasive and invasive Rb patients with respect to controls were depicted. Synonymic patterns of expression of metabolites were observed among noninvasive and invasive Rb patients; however, the extent of perturbation is quite distinct, with the effect being heightened in invasive Rb patients. ROC analysis outlined the efficacy of a panel of metabolites to differentiate distinct groups of noninvasive and invasive Rb patients from controls. The current study is also not devoid of limitations owing to its small sample size and heterogeneity. This warrants conducting this important piece of work with large patient cohorts in both categories (invasive as well as noninvasive Rb patients) as well as cross-validating the outcomes using other omics strategies. Such a metabolic landscape provides new avenues for clinical oncologists to tailor specific therapeutics for distinct Rb subgroups and avoid superfluous surgical procedures.

5. MATERIALS AND METHODS

5.1. Sample Collection. The study was conducted after seeking formal permission from the institutional Review Board committee (IRB) (LEC-BHR-P-01-21-575) of LVPEI (L.V. Prasad Eye Institute) and followed the principles underlying the Declaration of Helsinki. Written consent forms duly signed by the parents of the participating patients were attained. Rb was detected based on the clinical data obtained from the

https://doi.org/10.1021/acsomega.4c06014
ACS Omega 2024, 9, 40082−40094

patients using a combination of B-scan ultrasonography, orbital imaging, and examination under anesthesia. A total of 13 patients with unilateral Rb were included in this study. Noninvasive Rb was defined as an intraocular tumor limited to the retina with or without subretinal/vitreous seeds in which the eyes were salvaged with conservative treatment. Invasive Rb was defined as those eyes with advanced Rb who underwent primary enucleation and were confirmed to have at least one high-risk histopathology feature. The extent of invasion of tumor in invasive Rb patients was confirmed using histological examinations under a light microscope. The formalin (10%) fixed enucleated eyes from Rb patients were embedded into the paraffin wax using the standard protocol, and each section of the eye was stained using H&E (hematoxylin and eosin) staining. Slides were examined under a microscope to determine the high-risk histopathology features. High-risk histopathology features were defined as massive (≥3 mm) choroidal invasion, postlaminar optic nerve invasion, a combination of prelaminar/laminar optic nerve and minor (<3 mm) choroidal invasion, scleral invasion, and microscopic extrascleral extension. Blood samples were obtained from all patients, of which 4 had noninvasive Rb and 9 had invasive Rb. To perform comparative analysis, blood samples were also acquired from 6 patients with no reported signs of retina-related pathology. These 6 patients served as controls for this analytical study. All the blood samples (2 mL each) were processed in serum separator containers to obtain serum. Each blood sample was subjected to centrifugation for 15 min, at 2000*g*, while maintaining a temperature of 4 °C. Supernatant was separated from cellular debris (collected at the bottom of the tube) and was transferred into a microcentrifuge tube (1.5 mL) followed by storage at −80 °C. Experiments were performed using 300 μL serum aliquots that were lyophilized and stored at −80 °C.

5.2. NMR Sample Preparation and Data Acquisition. NMR samples were prepared as described previously.[20] In brief, samples were prepared by dissolving the lyophilized serum samples in 600 μL of sodium phosphate buffer (buffer strength: 20 mM, prepared in 100% D_2O, deuterium oxide) possessing 0.9% NaCl. Resultant NMR samples were subjected to centrifugation at 6708*g* for 5 min at room temperature before transferring 500 μL of it into a 5 mm NMR tube. 1 mM TSP (3-trimethylsilylpropanoic acid, 60 μL), a chemical shift indicator, was added in a coaxial tube to make a final concentration of 100 μM.[55] The TSP-containing tube was inserted into the NMR tube. ^{1}H NMR spectra were recorded for all of the serum samples at 298 K using a high-resolution Bruker NMR spectrometer (with 500 MHz ^{1}H frequency). The Carr−Purcell−Meiboom−Gill (cpmgpr1d) pulse sequence with water presaturation was used to attain the ^{1}H NMR spectra.[56,57] Spectral measurements for each serum sample were carried out using 20 ppm spectral width, 1536 acquisition scans, and a 4 s relaxation delay.

5.3. NMR Data Processing and Metabolite Profiling. Standard Fourier transformation processing was applied to manually process each CPMG-NMR spectrum in Bruker's TopSpin 4.0.6 software, specifically designed for processing NMR data. Calibration of each ^{1}H NMR spectrum was performed using a singlet peak at 0 ppm, which corresponds to the TSP signal. Further, each spectrum was subjected to phase and baseline corrections manually. The processed ^{1}H NMR spectrum was exported to a processor module of the ChenomX NMR suite 8.4 for further baseline corrections (Chenomx Inc., Edmonton, Canada). The assignment of peaks was carried out in the profiler module of Chenomx. Metabolites assigned to the respective peaks in Chenomx are based on the combination of chemical shift data contained in the human metabolome database (HMDB) and the 500 MHz NMR chemical shift database.[58] Further, a concentration data set representing the concentration of each metabolite estimated with respect to TSP was obtained using Chenomx. Metabolomics data has been submitted to the Indian Metabolome data archive (IMDA) of the Indian Biological Data Center (IBDC) (https://ibdc.dbtindia.gov.in/) and is accessible using accession ID: IMS_100010.

5.4. Statistical Analysis. Preprocessing of the metabolite concentration data set was performed using the combination of normalization parameters as described in our previous work.[20] All the statistical analysis was performed on the normalized metabolite concentration data set using the platform of metaboanalyst (V5.0).[59] Following data normalization, unsupervised principal component analysis was performed to obtain an overview of metabolomics data, detection of variable groups, and outliers.[60] Further, supervised partial least-squares (PLS) discriminant analysis (DA) was carried out for the identification of metabolites with the potential of discrimination among different Rb patients' groups. The performance of the PLS-DA score plot was assessed using a 5-fold cross-validation and permutation test. Qualitative assessment of the model was performed on the basis of a combination of three measures including R^2, Q^2, and prediction accuracy.[61] The variable importance of projection (VIP) score plot defining the group discriminating metabolites was generated based on the attained PLS-DA model.[62] Box cum Whisker plots of the top 20 metabolites possessing a VIP score greater than 1.0 were prepared. Heat maps were retrieved by employing an unsupervised hierarchical clustering methodology that is based on an algorithm known as Euclidean and Ward linkage. Fold change values of distinct metabolites among different pairs of groups (control vs noninvasive Rb patients, control vs invasive Rb patients, and noninvasive vs invasive Rb patients) were computed using a threshold value of 1.4 and *p*-value of 0.05.

The metabolite concentration data set was subjected to a pathway impact analysis module of Metaboanalyst.[59] This module integrates the outcomes of pathway enrichment and pathway topology analysis to identify the perturbed metabolic pathways. Metabolic connections among different pathways were identified based on an inbuilt *Homo sapiens* metabolic library in the KEGG pathway database.[63] Further, metabolites with high significance value and diagnostic potential were retrieved using receiver operating characteristic (ROC) curve analysis coupled with a student-*t* test, employing the biomarker analysis module of Metaboanalyst. The AUC (area under curve) of ROC curves was employed to identify the effective diagnostic value of metabolites. The support vector machine (SVM) algorithm was employed for the evaluation and ranking of all the important variables. *p*-Values (level of significance) were set at $p < 0.05$, and the categorical variables were expressed as percentage while continuous variables as mean ± SD.[64]

■ ASSOCIATED CONTENT

Supporting Information

The Supporting Information is available free of charge at https://pubs.acs.org/doi/10.1021/acsomega.4c06014.

https://doi.org/10.1021/acsomega.4c06014
ACS Omega 2024, 9, 40082−40094

Performance measurements for the PLS-DA model generated (Figure S1); Multivariate ROC analysis (Figure S2); Univariate ROC analysis (Figures S3, S4, and S5); and List of metabolic pathways perturbed (Tables S1, S2) (PDF)

AUTHOR INFORMATION

Corresponding Authors

Krishna Mohan Poluri − *Department of Biosciences and Bioengineering, Indian Institute of Technology Roorkee, Roorkee 247667 Uttarakhand, India; Centre for Nanotechnology, Indian Institute of Technology Roorkee, Roorkee 247667 Uttarakhand, India;* orcid.org/0000-0003-3801-7134; Phone: +91-1332-284779; Email: krishna.poluri@bt.iitr.ac.in

Swathi Kaliki − *The Operation Eyesight Universal Institute for Eye Cancer, L. V. Prasad Eye Institute, Hyderabad 500034 Telangana, India;* orcid.org/0000-0002-0800-9961; Email: kalikiswathi@yahoo.com

Author

Khushboo Gulati − *The Operation Eyesight Universal Institute for Eye Cancer, L. V. Prasad Eye Institute, Hyderabad 500034 Telangana, India; Brien Holden Eye Research Center, L. V. Prasad Eye Institute, Hyderabad 500034 Telangana, India*

Complete contact information is available at: https://pubs.acs.org/10.1021/acsomega.4c06014

Notes

The authors declare no competing financial interest.

ACKNOWLEDGMENTS

S.K., K.G., K.M.P. acknowledges the financial support by the SERB grant (CRG/2021/003236) and Hyderabad Eye Research Foundation L. V. Prasad Eye Institute (LVPEI). K.M.P. acknowledges the financial support of SERB-STAR grant (STR/2022/000008) from Govt. of India. The Authors acknowledge the use of a 500 MHz NMR spectrometer at the NMR facility of the Institute Instrumentation Center, IIT-Roorkee, India. The Authors acknowledge Dr. Saumya Jakati, pathologist, at L. V. Prasad Eye Institute (LVPEI), Hyderabad, Telangana, India, for providing histopathology data.

REFERENCES

(1) Rao, R.; Honavar, S. G. Retinoblastoma. *Indian J. Pediatr* **2017**, *84* (12), 937−944.

(2) Shields, C. L.; Shields, J. A. Diagnosis and management of retinoblastoma. *Cancer Control* **2004**, *11* (5), 317−27.

(3) Satyanarayana, L.; Asthana, S.; Preeti Labani, S. Childhood cancer incidence in India: a review of population-based cancer registries. *Indian Pediatr* **2014**, *51* (3), 218−220.

(4) Knudson, A. G., Jr Mutation and cancer: statistical study of retinoblastoma. *Proc. Natl. Acad. Sci. U. S. A.* **1971**, *68* (4), 820−3.

(5) Jagadeesan, M.; Khetan, V.; Mallipatna, A. Genetic perspective of retinoblastoma: From present to future. *Indian J. Ophthalmol* **2016**, *64* (5), 332−6.

(6) Singh, L.; Kashyap, S. Update on pathology of retinoblastoma. *Int. J. Ophthalmol* **2018**, *11* (12), 2011−2016.

(7) Chevez-Barrios, P.; Hurwitz, M. Y.; Louie, K.; Marcus, K. T.; Holcombe, V. N.; Schafer, P.; Aguilar-Cordova, C. E.; Hurwitz, R. L. Metastatic and nonmetastatic models of retinoblastoma. *Am. J. Pathol.* **2000**, *157* (4), 1405−12.

(8) Ancona-Lezama, D.; Dalvin, L. A.; Shields, C. L. Modern treatment of retinoblastoma: A 2020 review. *Indian J. Ophthalmol* **2020**, *68* (11), 2356−2365.

(9) Meel, R.; Radhakrishnan, V.; Bakhshi, S. Current therapy and recent advances in the management of retinoblastoma. *Indian J. Med. Paediatr Oncol* **2012**, *33* (2), 80−8.

(10) Lu, J. E.; Francis, J. H.; Dunkel, I. J.; Shields, C. L.; Yu, M. D.; Berry, J. L.; Kogachi, K.; Skalet, A. H.; Miller, A. K.; Santapuram, P. R.; Daniels, A. B.; Abramson, D. H. Metastases and death rates after primary enucleation of unilateral retinoblastoma in the USA 2007−2017. *Br J. Ophthalmol* **2019**, *103* (9), 1272−1277.

(11) Zhang, A.; Sun, H.; Wang, X. Serum metabolomics as a novel diagnostic approach for disease: a systematic review. *Anal Bioanal Chem.* **2012**, *404* (4), 1239−45.

(12) Boroughs, L. K.; DeBerardinis, R. J. Metabolic pathways promoting cancer cell survival and growth. *Nat. Cell Biol.* **2015**, *17* (4), 351−9.

(13) Schiliro, C.; Firestein, B. L. Mechanisms of Metabolic Reprogramming in Cancer Cells Supporting Enhanced Growth and Proliferation. *Cells* **2021**, *10* (5), 1056.

(14) Dey, P.; Kimmelman, A. C.; DePinho, R. A. Metabolic Codependencies in the Tumor Microenvironment. *Cancer Discov* **2021**, *11* (5), 1067−1081.

(15) Singh, A.; Prakash, V.; Gupta, N.; Kumar, A.; Kant, R.; Kumar, D. Serum Metabolic Disturbances in Lung Cancer Investigated through an Elaborative NMR-Based Serum Metabolomics Approach. *ACS Omega* **2022**, *7* (6), 5510−5520.

(16) More, T. H.; RoyChoudhury, S.; Christie, J.; Taunk, K.; Mane, A.; Santra, M. K.; Chaudhury, K.; Rapole, S. Metabolomic alterations in invasive ductal carcinoma of breast: A comprehensive metabolomic study using tissue and serum samples. *Oncotarget* **2018**, *9* (2), 2678−2696.

(17) Amiri-Dashatan, N.; Yekta, R. F.; Koushki, M.; Arefi Oskouie, A.; Esfahani, H.; Taheri, S.; Kazemian, E. Metabolomic study of serum in patients with invasive ductal breast carcinoma with LC-MS/MS approach. *Int. J. Biol. Markers* **2022**, *37* (4), 349−359.

(18) Faubert, B.; Solmonson, A.; DeBerardinis, R. J. Metabolic reprogramming and cancer progression. *Science* **2020**, *368* (6487), eaaw5473.

(19) Wolpaw, A. J.; Dang, C. V. Exploiting Metabolic Vulnerabilities of Cancer with Precision and Accuracy. *Trends Cell Biol.* **2018**, *28* (3), 201−212.

(20) Gulati, K.; Manukonda, R.; Kairamkonda, M.; Kaliki, S.; Poluri, K. M. Serum Metabolomics of Retinoblastoma: Assessing the Differential Serum Metabolic Signatures of Unilateral and Bilateral Patients. *ACS Omega* **2023**, *8* (50), 48233−48250.

(21) Suresh Babu, V.; Dudeja, G.; Sa, D.; Bisht, A.; Shetty, R.; Heymans, S.; Guha, N.; Ghosh, A. Lack of Retinoblastoma Protein Shifts Tumor Metabolism from Glycolysis to OXPHOS and Allows the Use of Alternate Fuels. *Cells* **2022**, *11* (20), 3182.

(22) Naik, A.; Decock, J. Lactate Metabolism and Immune Modulation in Breast Cancer: A Focused Review on Triple Negative Breast Tumors. *Front Oncol* **2020**, *10*, 598626.

(23) Sitter, B.; Forsmark, A.; Solheim, O. Elevated Serum Lactate in Glioma Patients: Associated Factors. *Front Oncol* **2022**, *12*, 831079.

(24) Brizel, D. M.; Schroeder, T.; Scher, R. L.; Walenta, S.; Clough, R. W.; Dewhirst, M. W.; Mueller-Klieser, W. Elevated tumor lactate concentrations predict for an increased risk of metastases in head-and-neck cancer. *Int. J. Radiat Oncol Biol. Phys.* **2001**, *51* (2), 349−53.

(25) Feron, O. Pyruvate into lactate and back: from the Warburg effect to symbiotic energy fuel exchange in cancer cells. *Radiother Oncol* **2009**, *92* (3), 329−33.

(26) Li, X.; Yang, Y.; Zhang, B.; Lin, X.; Fu, X.; An, Y.; Zou, Y.; Wang, J. X.; Wang, Z.; Yu, T. Lactate metabolism in human health and disease. *Signal Transduct Target Ther* **2022**, *7* (1), 305.

(27) Gao, Y.; Zhou, H.; Liu, G.; Wu, J.; Yuan, Y.; Shang, A. Tumor Microenvironment: Lactic Acid Promotes Tumor Development. *J. Immunol Res.* **2022**, *2022*, 3119375.

(28) Kuo, C. C.; Wu, J. Y.; Wu, K. K. Cancer-derived extracellular succinate: a driver of cancer metastasis. *J. Biomed Sci.* **2022**, *29* (1), 93.
(29) Wu, J. Y.; Huang, T. W.; Hsieh, Y. T.; Wang, Y. F.; Yen, C. C.; Lee, G. L.; Yeh, C. C.; Peng, Y. J.; Kuo, Y. Y.; Wen, H. T.; Lin, H. C.; Hsiao, C. W.; Wu, K. K.; Kung, H. J.; Hsu, Y. J.; Kuo, C. C. Cancer-Derived Succinate Promotes Macrophage Polarization and Cancer Metastasis via Succinate Receptor. *Mol. Cell* **2020**, *77* (2), 213−227.
(30) Gray, L. R.; Tompkins, S. C.; Taylor, E. B. Regulation of pyruvate metabolism and human disease. *Cell. Mol. Life Sci.* **2014**, *71* (14), 2577−604.
(31) Viswanath, P.; Radoul, M.; Izquierdo-Garcia, J. L.; Luchman, H. A.; Gregory Cairncross, J.; Pieper, R. O.; Phillips, J. J.; Ronen, S. M. Mutant IDH1 gliomas downregulate phosphocholine and phosphoethanolamine synthesis in a 2-hydroxyglutarate-dependent manner. *Cancer Metab* **2018**, *6*, 3.
(32) Saito, R. F.; Andrade, L. N. S.; Bustos, S. O.; Chammas, R. Phosphatidylcholine-Derived Lipid Mediators: The Crosstalk Between Cancer Cells and Immune Cells. *Front Immunol* **2022**, *13*, 768606.
(33) Li, Z.; Vance, D. E. Phosphatidylcholine and choline homeostasis. *J. Lipid Res.* **2008**, *49* (6), 1187−94.
(34) Pilley, S. E.; Hennequart, M.; Vandekeere, A.; Blagih, J.; Legrave, N. M.; Fendt, S. M.; Vousden, K. H.; Labuschagne, C. F. Loss of attachment promotes proline accumulation and excretion in cancer cells. *Sci. Adv.* **2023**, *9* (36), No. eadh2023.
(35) Mattaini, K. R.; Sullivan, M. R.; Vander Heiden, M. G. The importance of serine metabolism in cancer. *J. Cell Biol.* **2016**, *214* (3), 249−57.
(36) Amelio, I.; Cutruzzola, F.; Antonov, A.; Agostini, M.; Melino, G. Serine and glycine metabolism in cancer. *Trends Biochem. Sci.* **2014**, *39* (4), 191−8.
(37) Yi, H.; Talmon, G.; Wang, J. Glutamate in cancers: from metabolism to signaling. *J. Biomed Res.* **2020**, *34* (4), 260−270.
(38) Kohe, S.; Brundler, M. A.; Jenkinson, H.; Parulekar, M.; Wilson, M.; Peet, A. C.; McConville, C. M.; Children's, C.; Leukaemia, G. Metabolite profiling in retinoblastoma identifies novel clinicopathological subgroups. *Br. J. Cancer* **2015**, *113* (8), 1216−24.
(39) Lee, M.; Schwab, C.; McGeer, P. L. Astrocytes are GABAergic cells that modulate microglial activity. *Glia* **2011**, *59* (1), 152−65.
(40) Le Meur, K.; Mendizabal-Zubiaga, J.; Grandes, P.; Audinat, E. GABA release by hippocampal astrocytes. *Front Comput. Neurosci* **2012**, *6*, 59.
(41) Kozlov, A. S.; Angulo, M. C.; Audinat, E.; Charpak, S. Target cell-specific modulation of neuronal activity by astrocytes. *Proc. Natl. Acad. Sci. U. S. A.* **2006**, *103* (26), 10058−63.
(42) Jow, F.; Chiu, D.; Lim, H. K.; Novak, T.; Lin, S. Production of GABA by cultured hippocampal glial cells. *Neurochem. Int.* **2004**, *45* (2−3), 273−83.
(43) Huang, D.; Wang, Y.; Thompson, J. W.; Yin, T.; Alexander, P. B.; Qin, D.; Mudgal, P.; Wu, H.; Liang, Y.; Tan, L.; Pan, C.; Yuan, L.; Wan, Y.; Li, Q. J.; Wang, X. F. Cancer-cell-derived GABA promotes beta-catenin-mediated tumour growth and immunosuppression. *Nat. Cell Biol.* **2022**, *24* (2), 230−241.
(44) Tian, J.; Kaufman, D. L. The GABA and GABA-Receptor System in Inflammation, Anti-Tumor Immune Responses, and COVID-19. *Biomedicines* **2023**, *11* (2), 254.
(45) Young, S. Z.; Bordey, A. GABA's control of stem and cancer cell proliferation in adult neural and peripheral niches. *Physiology (Bethesda)* **2009**, *24*, 171−85.
(46) Satriano, J. Arginine pathways and the inflammatory response: interregulation of nitric oxide and polyamines: review article. *Amino Acids* **2004**, *26* (4), 321−9.
(47) Soda, K. The mechanisms by which polyamines accelerate tumor spread. *J. Exp Clin Cancer Res.* **2011**, *30* (1), 95.
(48) Muthukumaran, S.; Bhuvanasundar, R.; Umashankar, V.; Sulochana, K. N. Insights on ornithine decarboxylase silencing as a potential strategy for targeting retinoblastoma. *Biomed Pharmacother* **2018**, *98*, 23−28.
(49) Xie, H.; Zhang, K.; Wei, Y.; Ruan, G.; Zhang, H.; Li, S.; Song, Y.; Chen, P.; Liu, L.; Wang, B.; Shi, H. The association of serum betaine concentrations with the risk of new-onset cancers: results from two independent nested case-control studies. *Nutr Metab (Lond)* **2023**, *20* (1), 46.
(50) Ueland, P. M. Choline and betaine in health and disease. *J. Inherit Metab Dis* **2011**, *34* (1), 3−15.
(51) de Vogel, S.; Ulvik, A.; Meyer, K.; Ueland, P. M.; Nygard, O.; Vollset, S. E.; Tell, G. S.; Gregory, J. F., 3rd; Tretli, S.; Bjorge, T. Sarcosine and other metabolites along the choline oxidation pathway in relation to prostate cancer-a large nested case-control study within the JANUS cohort in Norway. *Int. J. Cancer* **2014**, *134* (1), 197−206.
(52) Huang, J. Y.; Luu, H. N.; Butler, L. M.; Midttun, O.; Ulvik, A.; Wang, R.; Jin, A.; Gao, Y. T.; Tan, Y.; Ueland, P. M.; Koh, W. P.; Yuan, J. M. A prospective evaluation of serum methionine-related metabolites in relation to pancreatic cancer risk in two prospective cohort studies. *Int. J. Cancer* **2020**, *147* (7), 1917−1927.
(53) Butler, L. M.; Arning, E.; Wang, R.; Bottiglieri, T.; Govindarajan, S.; Gao, Y. T.; Yuan, J. M. Prediagnostic levels of serum one-carbon metabolites and risk of hepatocellular carcinoma. *Cancer Epidemiol Biomarkers Prev* **2013**, *22* (10), 1884−93.
(54) Reichard, C. A.; Naelitz, B. D.; Wang, Z.; Jia, X.; Li, J.; Stampfer, M. J.; Klein, E. A.; Hazen, S. L.; Sharifi, N. Gut Microbiome-Dependent Metabolic Pathways and Risk of Lethal Prostate Cancer: Prospective Analysis of a PLCO Cancer Screening Trial Cohort. *Cancer Epidemiol Biomarkers Prev* **2022**, *31* (1), 192−199.
(55) Gulati, K.; Sarkar, S.; Poluri, K. M. Metabolomics analysis of complex biological specimens using nuclear magnetic resonance spectroscopy. *Metabolomics* **2021**, *159*, 155−171.
(56) Nagana Gowda, G. A.; Raftery, D. NMR-Based Metabolomics. *Adv. Exp. Med. Biol.* **2021**, *1280*, 19−37.
(57) Crook, A. A.; Powers, R. Quantitative NMR-Based Biomedical Metabolomics: Current Status and Applications. *Molecules* **2020**, *25* (21), 5128.
(58) Wishart, D. S.; Guo, A.; Oler, E.; Wang, F.; Anjum, A.; Peters, H.; Dizon, R.; Sayeeda, Z.; Tian, S.; Lee, B. L.; Berjanskii, M.; Mah, R.; Yamamoto, M.; Jovel, J.; Torres-Calzada, C.; Hiebert-Giesbrecht, M.; Lui, V. W.; Varshavi, D.; Varshavi, D.; Allen, D.; Arndt, D.; Khetarpal, N.; Sivakumaran, A.; Harford, K.; Sanford, S.; Yee, K.; Cao, X.; Budinski, Z.; Liigand, J.; Zhang, L.; Zheng, J.; Mandal, R.; Karu, N.; Dambrova, M.; Schioth, H. B.; Greiner, R.; Gautam, V. HMDB 5.0: the Human Metabolome Database for 2022. *Nucleic Acids Res.* **2022**, *50* (D1), D622−D631.
(59) Pang, Z.; Chong, J.; Zhou, G.; de Lima Morais, D. A.; Chang, L.; Barrette, M.; Gauthier, C.; Jacques, P. E.; Li, S.; Xia, J. MetaboAnalyst 5.0: narrowing the gap between raw spectra and functional insights. *Nucleic Acids Res.* **2021**, *49* (W1), W388−W396.
(60) Xia, J.; Psychogios, N.; Young, N.; Wishart, D. S. MetaboAnalyst: a web server for metabolomic data analysis and interpretation. *Nucleic Acids Res.* **2009**, *37*, 652−660.
(61) Chong, J.; Wishart, D. S.; Xia, J. Using MetaboAnalyst 4.0 for Comprehensive and Integrative Metabolomics Data Analysis. *Curr. Protoc Bioinformatics* **2019**, *68* (1), No. e86.
(62) Kairamkonda, M.; Sharma, M.; Gupta, P.; Poluri, K. M. Overexpression of bacteriophage T4 and T7 endolysins differentially regulate the metabolic fingerprint of host Escherichia coli. *Int. J. Biol. Macromol.* **2022**, *221*, 212−223.
(63) Kanehisa, M.; Furumichi, M.; Tanabe, M.; Sato, Y.; Morishima, K. KEGG: new perspectives on genomes, pathways, diseases and drugs. *Nucleic Acids Res.* **2017**, *45* (D1), D353−D361.
(64) Xia, J.; Broadhurst, D. I.; Wilson, M.; Wishart, D. S. Translational biomarker discovery in clinical metabolomics: an introductory tutorial. *Metabolomics* **2013**, *9* (2), 280−299.

https://doi.org/10.1021/acsomega.4c06014
ACS Omega 2024, 9, 40082−40094